Remote Sensing of Environment 146 (2014) 87–96

Contents lists available at ScienceDirect

Remote Sensing of Environment

journal homepage: www.elsevier.com/locate/rse

Remote sensing of assimilation number for marine phytoplankton

S. Saux Picart [a,*], S. Sathyendranath [a], M. Dowell [b], T. Moore [c], T. Platt [a]

[a] Plymouth Marine Laboratory, Prospect Place, The Hoe, PL13DH Plymouth, United Kingdom
[b] Joint Research Centre, via Enrico Fermi 2749, 21027 Ispra, Italy
[c] University of New Hampshire, Morse Hall, 39 College Road, Durham, NH 03824, USA

ARTICLE INFO

Article history:
Received 1 November 2012
Received in revised form 4 October 2013
Accepted 31 October 2013
Available online 15 December 2013

Keywords:
Marine primary production
Photosynthetic parameters
Remote sensing
Assimilation number

ABSTRACT

Estimating primary production at large spatial scales is key to our understanding of the global carbon cycle. Algorithms to estimate primary production are well established and have been used in many studies with success. One of the key parameters in these algorithms is the chlorophyll-normalised production rate under light saturation (referred to as the light saturation parameter or the assimilation number). It is known to depend on temperature, light history and nutrient conditions, but assigning a magnitude to it at particular space-time points is difficult. In this paper, we explore two models to estimate the assimilation number at the global scale from remotely-sensed data that combine methods to estimate the carbon-to-chlorophyll ratio and the maximum growth rate of phytoplankton. The inputs to the algorithms are the surface concentration of chlorophyll, sea-surface temperature, photosynthetically-active radiation at the surface of the sea, sea surface nutrient concentration and mixed-layer depth. A large database of in situ estimates of the assimilation number is used to develop the models and provide elements of validation. The comparisons with in situ observations are promising and global maps of assimilation number are produced.

© 2013 Elsevier Inc. All rights reserved.

1. Introduction

An important application of ocean-colour data has been the computation of marine primary production at the global scale (Antoine, André, & Morel, 1996; Antoine & Morel, 1996; Behrenfeld & Falkowski, 1997; Chavez, Messié, & Pennington, 2011; Friedrichs et al., 2009; Longhurst, Sathyendranath, Platt, & Caverhill, 1995). Typically, these computations use chlorophyll concentration derived from ocean colour as the state variable, although alternate approaches that use phytoplankton carbon rather than chlorophyll concentration have also been proposed (Behrenfeld, Boss, Siegel, & Shea, 2005). All these models require auxiliary information on light available at the sea surface, which is then combined with light-penetration models to compute the light available at depth for photosynthesis. A key step in the computations, and a non-trivial one, is the assignment of the model parameters required to estimate the photosynthetic response of phytoplankton to available or absorbed light.

Longhurst et al. (1995) and Platt and Sathyendranath (1999) proposed delineation of ecological provinces in the ocean as a template for extrapolating sparse in situ measurements of photosynthesis–irradiance parameters to the global ocean. Platt et al. (2008) developed the so-called nearest-neighbour methodology to assign, for each pixel (characterised by chlorophyll concentration and temperature), values of these parameters representative of similar local environmental conditions. Both of these methodologies rely on the availability of a database of photosynthesis–irradiance parameter measurements on which the extrapolation is based.

In the remote sensing context, the methods described above can be placed in a more generic categorisation of different options for parameter assignment for primary-production models (Platt & Sathyendranath, 1999). Specifically, the ecological-province-based approach may be termed as a piecewise-constant approach to parameter assignment (Longhurst et al., 1995). There are however alternative approaches which include the continuous method, where the assignments are based on some other empirical or parametric relation to other variables amenable to remote sensing (as in the case of the nearest-neighbour method, Platt et al., 2008). Another approach is the piecewise-continuous method, which is a combination of the two previous approaches (e.g. Huot, Babin, & Bruyant, 2013). In the current paper we consider a method that falls in the category of the continuous approach for estimating the assimilation number. Each method has its own inherent advantages and disadvantages. In the case of the continuous approach the advantages lie in its applicability in more dynamic regions, where the piecewise approach would lead to discontinuities in the production field, and its applicability at regional and basin scales, so long as the proposed approach is valid over the dynamic range of variability represented in the regions considered.

Some authors have linked the assimilation number to temperature (Eppley, 1972) and have shown that it is possible to use a temperature relationship in some particular conditions (shallow coastal and estuarine areas) as a basis for assigning it. The assimilation number has also been shown to be correlated with the available light (Finenko, Churilova, Sosik, & Basturk, 2002; Geider, 1987), nutrients (Harrison &

* Corresponding author.
E-mail address: s.saux-picart@pml.ac.uk (S. Saux Picart).

0034-4257/$ – see front matter © 2013 Elsevier Inc. All rights reserved.
http://dx.doi.org/10.1016/j.rse.2013.10.032

Platt, 1980) and depth (Marañón & Holligan, 1999), which may be a proxy for both light and nutrient.

In this study we explore two options to estimate the assimilation number from combinations of easily-measured environmental variables. The first one is a global implementation of the model of Cloern, Grenz, and Vidergar-Lucas (1995). The second is based on the model of Sathyendranath et al. (2009) for estimating the carbon-to-chlorophyll ratio of phytoplankton, which is extended here to estimate the assimilation number. The choice of the two approaches was dictated by the goal of applying the methods globally, preferably using satellite data: both approaches presented here require only a small set of input variables that are readily available at the global scale. From the perspective of implementation, both models require temperature and light as inputs. The main difference between them is that the Cloern et al. (1995) model requires nitrate fields, whereas the other approach presented here requires chlorophyll fields instead of nitrate fields.

2. Material and methods

2.1. Approach

Marine primary production at a particular time and depth can be computed using photosynthesis-light models, which incorporate the parameters of the photosynthesis–irradiance curve (P–E curve). Integration over time and depth enables estimation of daily water column production. Although a number of variants of photosynthesis–light models exist in the literature, and regardless of the formalism adopted to describe the dependence of photosynthesis on available light, the relationships may all be expressed in the general form:

$$P^B(t,z) = P^B\left(E(t,z);\alpha^B,P^B_{\mathrm{m}}\right), \tag{1}$$

where P stands for primary production, E is irradiance, t is time and z is depth. The parameters of the model are α^B, the initial slope of the photosynthesis–irradiance curve as light tends to zero, and P^B_{m}, the assimilation number, which is a measure of the asymptotic maximum production under light-saturating conditions. Superscript B indicates normalisation to chlorophyll biomass B. The above equation states simply that chlorophyll-normalised production at a particular depth and time can be computed if we know the light available and the two parameters of the P–E curve. A third parameter would be needed under conditions of photo-inhibition. In photosynthesis-light experiments, dark respiration is corrected for, such that the model yields net primary production.

The photosynthesis–irradiance parameters have a central role in primary production models, and this study focuses on one of the parameters: the assimilation number, P^B_{m}, which may be defined as the asymptotic maximum rate of change in phytoplankton carbon due to net primary production, per unit chlorophyll concentration:

$$P^B_{\mathrm{m}} = \frac{1}{B}\frac{\mathrm{d}C_p}{\mathrm{d}t}\Big|_{\max}, \tag{2}$$

where C_p is the phytoplankton carbon concentration. It is useful to establish the relationship between P^B_{m} and maximum realised growth rate, μ_{m}, defined as:

$$\mu_{\mathrm{m}} = \frac{1}{C_p}\frac{\mathrm{d}C_p}{\mathrm{d}t}\Big|_{\max}. \tag{3}$$

Comparing Eqs. (2) and (3) we see that:

$$P^B_{\mathrm{m}} = \chi\mu_{\mathrm{m}}, \tag{4}$$

where χ is the carbon-to-chlorophyll ratio of phytoplankton.

The objective of our work is to establish methods to estimate P^B_{m} from environmental variables that are readily available, preferably through remote sensing. We explore two options here: both are based on existing methods to estimate χ and μ_{m}.

2.1.1. Model of assimilation number based on light, temperature and nutrients (LTN model)

This approach combines the chlorophyll-to-carbon model developed by Cloern et al. (1995) and the maximum growth rate as a function of temperature proposed by Eppley (1972).

Cloern et al. (1995) provided an empirical relationship linking the chlorophyll-to-carbon ratio (in phytoplankton) to temperature, average daily irradiance in the mixed layer and nutrient-limited growth rate:

$$B:\mathrm{C}_p = \frac{1}{\chi} = 0.003 + 0.0154exp(0.05T)exp(-0.059E)\mu', \tag{5}$$

where T is the temperature (°C), E is the daily irradiance (photosynthetically-active radiation, PAR) averaged over the mixed-layer depth (mol quantan $\mathrm{m}^{-2}\,\mathrm{d}^{-1}$) and $\mu' = N/(N + k_N)$ is the nutrient-limited growth rate, with N being the concentration of the most limiting nutrient (taken here to be nitrate) and k_N the half-saturation constant for that nutrient.

Combining Eqs. (4) and (5), the LTN model for the assimilation number can be expressed as:

$$P^{B,\mathrm{LTN}}_{\mathrm{m}} = \left[0.003 + 0.0154exp(0.05T)exp(-0.059E)\mu'\right]^{-1}\mu_{\mathrm{m}}. \tag{6}$$

This model can be implemented if we know the maximum growth rate μ_{m}, the temperature, the nutrient concentration, the average light in the mixed layer and the half-saturation constant k_N, for which Cloern et al. (1995) have used a value of 1 μM in their computations. On the other hand, Harrison, Harris, and Irwin (1996) have reported that k_N is positively correlated with nitrate concentration, with a lower limit around 0.01 to 0.02 μM. Combining these, k_N may be modelled as:

$$k_N = \begin{cases} 0.01, & N \le 0.01 \\ N, & 0.01 < N \le 1 \\ 1, & 1 < N \end{cases}. \tag{7}$$

To compute the maximum growth rate, we use the maximum temperature-dependent growth rate defined by Eppley (1972), μ^E_{m}, multiplied by a nutrient-limitation term, μ':

$$\mu_{\mathrm{m}} = \mu^E_{\mathrm{m}}\,\mu' = 0.851\left(1.066^T\right)\frac{\ln 2}{24}\left[\frac{N}{N+k_N}\right], \tag{8}$$

where the factor ln 2/24 accounts for the transformation from doubling time to hourly growth rate.

2.1.2. Model of assimilation number based on light, temperature and chlorophyll biomass (LTB model)

Nutrients are not directly observable by satellites, and for remote sensing of P^B_{m} we seek other options for a predictive environmental variable. Here we explore the use of chlorophyll biomass B instead of nutrients. Several studies have highlighted the relationship between chlorophyll concentration and phytoplankton cell size (see for example Brewin et al., 2010; Hirata, Aiken, Hardman-Mountford, Smyth, & Barlow, 2008), which is an important determinant of physiological rates. We begin with the expression for χ, the carbon-to-chlorophyll ratio, proposed by Sathyendranath et al. (2009):

$$\chi = \frac{1}{B}10^{(1.81+0.63log_{10}(B))}. \tag{9}$$

This expression, as pointed out by the authors, yields an upper bound on the phytoplankton carbon concentration, but does not

account for modulations of the quantity due to variations in available light or temperature. We therefore add these effects to the above equation, as follow:

$$\chi = \frac{1}{B} 10^{(1.81+0.63\log_{10}(B))}(1+n_1 T)(1+n_2 E), \quad (10)$$

where n_1 and n_2 are two parameters to be determined. With this expression for χ, the estimate for P_m^B in the LTB model becomes:

$$P_m^{B,\mathrm{LTB}} = \left[\frac{1}{B} 10^{(1.81+0.63log_{10}(B))}(1+n_1 T)(1+n_2 E)\right]\mu_m, \quad (11)$$

where μ_m is, in this model, the product of the maximum temperature-dependent growth rate given by the same temperature-dependent growth term of Eppley (1972) as in Eq. (8) (μ_m^E) and a nutrient limitation term which is parameterised here as a function of chlorophyll as a proxy for nutrient, $\mu'' = B/(B + k_B)$:

$$\mu_m = \mu_m^E \, \mu'' = 0.851\left(1.066^T\right)\frac{\ln 2}{24}\left[\frac{B}{B+k_B}\right], \quad (12)$$

where k_B is the half-saturation constant for the chlorophyll term. To the extent that any observed chlorophyll concentration is evidence of the prior availability of nutrients used to produce it, and perhaps also to maintain it, we may consider that chlorophyll, within a conversion factor, provides a lower bound on nutrient supply. In the case where the nutrient supply is in excess of demand, nutrient concentration is no longer a critical factor in the estimation of the assimilation number.

The advantage of this approach is the ready availability of surface chlorophyll concentration fields directly from remote sensing.

2.2. Determining average light in the mixed layer

Both the LTN and the LTB approaches require information on daily, average light in the mixed layer. The photosynthetically-active radiation at the sea surface may be obtained from in situ measurements or derived from satellite observations. However, the variable of interest for our purpose is the daily irradiance averaged over the mixed-layer depth.

To estimate this quantity, we used a spectrally-resolved model of underwater light-transmission (Sathyendranath & Platt, 1988) and the chlorophyll concentration in the mixed layer to determine K_d, the diffuse attenuation coefficient for photosynthetically-active radiation for the layer extending from the surface to the base of the mixed layer, assuming clear skies. Given K_d, the daily average irradiance in the mixed layer (E) can be computed as (see for example, Cloern et al., 1995):

$$E = \frac{E_0}{K_d Z_m}(1 - exp(-K_d Z_m)), \quad (13)$$

where E_0 is the daily irradiance at the surface, and Z_m is the mixed-layer depth.

2.3. Data

A large database of in situ data has been used in this study. Earlier versions of this database have been described by Bouman, Platt, Sathyendranath, and Stuart (2005) and Sathyendranath et al. (2009). It is based on a number of cruises from 1996 to 2004.

The database holds 680 measurements of the assimilation number. Corresponding measurements of mixed-layer depth, photosynthetically-active radiation and nitrate concentration were not always available in the dataset. Missing information was filled in by climatological data (see Table 1) using a simple spatial and temporal matchup procedure. For surface irradiance, we used the climatology of daily photosynthetically-active radiation at the surface derived from the SeaWiFS satellite data courtesy of NASA (http://oceancolor.gsfc.nasa.gov/) for the corresponding day of year and location. For nitrate concentration and mixed-layer depth, monthly climatologies from the World Ocean Atlas (Garcia, Locarnini, Boyer, & Antonov, 2006) and from de Boyer Montégut, Madec, Fisher, Lazar, and Iudicone (2004) respectively were used and the temporal matchup was therefore made on a monthly basis. Overall, most records lacked measurement of surface PAR and mixed-layer depth. Only the records for which we have been able to fill in missing data were used.

Table 1
Number of data records filled in with climatologies of photosynthetically-active radiation (PAR), nitrate (NO_3) and mixed-layer depth (MLD). N is the total number of records containing the assimilation number.

Area	N	Records filled in with climatology of			
		PAR	NO_3	MLD	PAR, NO_3 or MLD
North West Atlantic	461	310	298	308	416
North East Atlantic	18	18	2	18	18
Tropics & Chile	201	201	28	201	201
All	680	529	328	527	635

The data cover a variety of oceanic conditions ranging from high latitudes to the tropics (see Fig. 1). Most of the data (650 samples) came from the North West Atlantic and the Arabian Sea. The remaining data came from the middle of the North East Atlantic Ocean (off the European shelf), the Gulf of Mexico and off the Chilean coast. Table 1 gives the number of measurements in each region and the number of ancillary data needed to complete the dataset.

2.4. Optimisation and validation of the LTB model

The LTB model has three unknown parameters that need to be determined. A least squares optimisation technique (Sequential Least Squares Programming function from the Scipy Python module) was used to minimise the root-mean-square error between the measured and estimated assimilation number.

In a first experiment the set of available data (described in Section 2.3) was divided in two. One part, containing two thirds of the data, randomly sampled, was used to determine the parameters by the method described above, and the remaining part was used for validation. The first line of Table 2 shows the results of the optimisation step with associated statistics (when the LTB model is compared with the measurements against which it is optimised). The second line of Table 2 provides the same statistics when the LTB model is compared with the measurements not used in the optimisation step. The validation exhibits similar statistics to the optimisation step, demonstrating the robustness of the model.

In a second experiment, to estimate the confidence interval on the parameters, we used the bootstrapping methodology (Sheskin, 2007). The principle of this method is to run a large number (in our case we choose 1000) of optimizations using each time a different, randomly-selected subsample of the original dataset. The result from the thousand optimizations is a frequency distribution for each parameter, from which we select the 5th and the 95th percentile to define the 90% confidence interval. For this step all available data were used. Table 2 (third line) provides the final set of parameters (in bold, which we use in the subsequent analysis), associated confidence intervals and statistics of the comparison between the LTB model and measurements.

3. Analysis of model results

This section provides a detailed analysis of the two models, their sensitivity and responses to environmental variables.

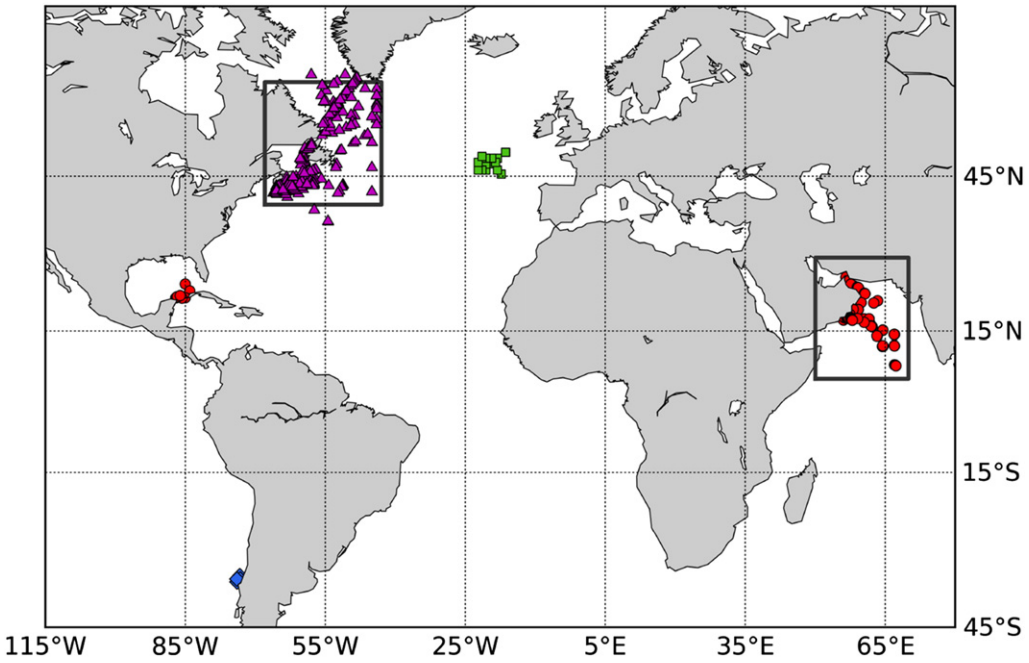

Fig. 1. Available measurements of assimilation number. Symbols differentiate the regions: North West Atlantic (magenta triangles); Tropics (red discs); North East Atlantic (green squares); Off Chile (blue diamonds). The boxes are the two areas used in Section 4.

3.1. Sensitivity of the models to environmental variables

Fig. 2 shows the sensitivity of computed P^B_m to the environmental variables on which it depends according to the LTN and the LTB models, for selected values of nutrient N and chlorophyll B, and ranges of temperature T and light E.

According to Fig. 2, P^B_m decreases with increasing nutrient or chlorophyll concentration respectively for the LTN and LTB models. The P^B_m computed using the LTN model increases monotonically with temperature (Fig. 2a–c). On the other hand, the result of the LTB model increases with temperature for low temperature ($T < 25$ °C) and then decreases with further increase in temperature (Fig. 2d–f). The decrease in P^B_m at higher temperatures is consistent with the observations of Bouman et al. (2005).

Both models show P^B_m increasing with average light in the mixed layer (Fig. 2). However, the LTN model is weakly sensitive to light at low nutrient concentration (Fig. 2a) and becomes strongly sensitive to light at high nutrient concentration (Fig. 2c). The LTB model remains sensitive to light irrespective of the chlorophyll concentration.

It is interesting to note that at low nutrient concentrations, the LTN model is highly sensitive to temperature and almost insensitive to light, whilst at high nutrient concentration one can observe the opposite behaviour. On the other hand the LTB model maintains its sensitivity to both temperature and light whatever the chlorophyll concentration might be. This can have a profound impact on the results, particularly where large variations or gradients of nutrient concentration are observed (coastal areas for example).

For a better insight into the response of the models to variations in environmental variables, we represent the carbon-to-chlorophyll (χ) component of each model in Fig. 3. In the LTB model, χ (Fig. 3a) decreases as chlorophyll concentration increases ranging from 100 to 600 gC (g Chl)$^{-1}$ at low chlorophyll values to around 20 to 70 gC (g Chl)$^{-1}$ when chlorophyll concentration is high (10 mg m^{-3}). On the other hand, the parameterisation used in the LTN model yields χ (Fig. 3b) ranging from 200 to 300 gC (g Chl)$^{-1}$ at low nutrient levels to 20 to 150 gC (g Chl)$^{-1}$ when the nutrient concentration is high (10 μM). It also shows strong sensitivity to light and temperature when nutrient concentration is high. Fig. 4 shows the evolution of the maximum realised growth rate term in both models. The thick black line is μ^E_m used in both the LTN and the LTB models and the dotted lines are the μ_m term, for three chlorophyll or nutrient concentrations. As the chlorophyll concentration decreases, the nutrient limitation term becomes stronger, and at a concentration of 0.01 mg m^{-3} temperature plays a non significant role on the maximum realised growth rate in the LTB model, but the sensitivity to temperature remains relatively high in the LTN model at low nitrate levels.

3.2. Comparison between LTN and LTB models

Fig. 5 shows modelled assimilation number based on LTN and LTB models plotted against corresponding in situ estimates, and the statistics associated with these figures are shown in Table 3.

The LTN model is relatively more scattered with a root mean square error (RMSE) of 2.265 mg C mg Chl^{-1} h^{-1}, but the cloud of points is

Table 2
Table summarising the optimisation/validation results as well as the determination of the confidence interval (in brackets) on the final set of parameters of the LTB model (units of the parameters: n_1[(° C)$^{-1}$]; n_2[(mol quanta m^{-2} d^{-1})$^{-1}$]; k_B[mg m^{-3}]). Bias, root mean square error (RMSE), Spearman correlation coefficient (r) and associated two-sided p-value are shown.

		n_1	n_2	k_B	Bias	RMSE	r	p-Value
	Optimisation	−0.023	0.037	0.094	0.047	1.785	0.41	0.087
LTB	Validation	–	–	–	0.095	1.586	0.50	0.099
	Bootstrap	**−0.023**	**0.035**	**0.075**	−0.43	1.898	0.45	0.050
		(−0.025,−0.021)	(0.027, 0.044)	(0.039, 0.114)				
LTN	Validation	–	–	–	−0.889	2.265	0.37	0.06

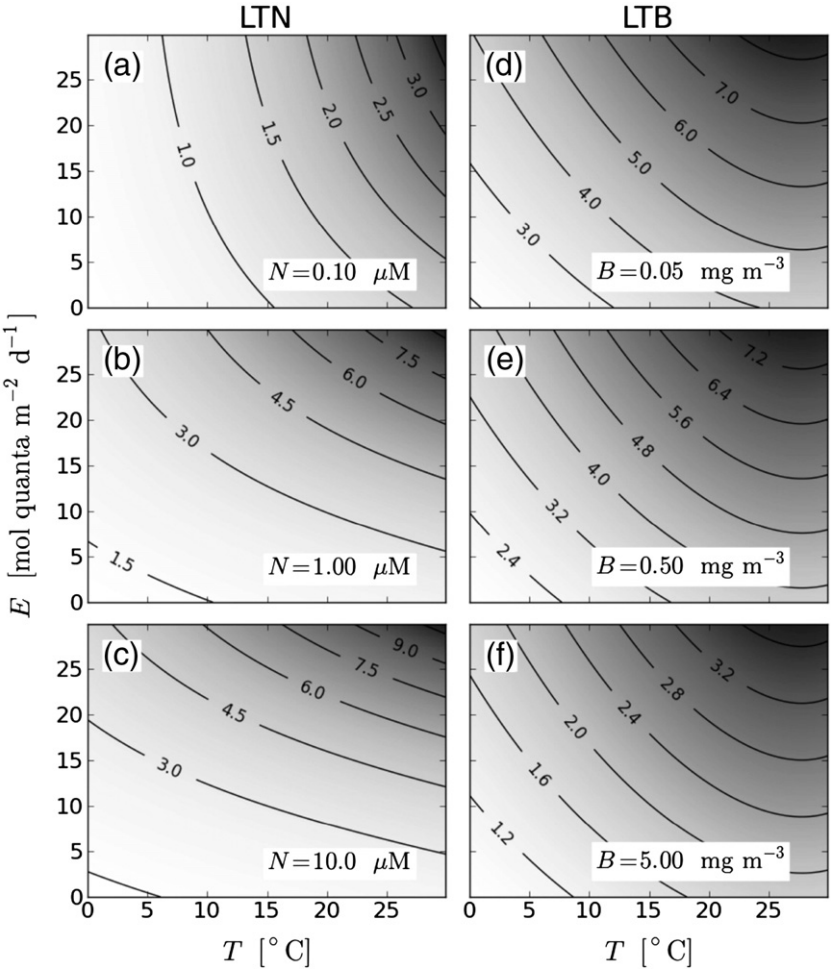

Fig. 2. Sensitivity of the LTN model (panels a–c) and LTB model (panels d–f) to environmental variables.

centred on the identity line. The performance of the LTB model is slightly better, with a lower bias and RMSE and a higher correlation coefficient. But we have to bear in mind that the LTB model was optimised against the data presented in Fig. 5, whereas the LTN model parameters are derived from completely independent studies (Cloern et al., 1995; Eppley, 1972). It is remarkable that the LTN model based on culture measurements performs so well at predicting the assimilation number from field observations made in a variety of natural environmental conditions in the open ocean and in coastal waters.

When the results are broken down by region (Fig. 5 and Table 3), the North West Atlantic is where both models perform best, whereas the results for the other regions show higher bias and higher RMSE. However, the correlation for the North East Atlantic is the highest. Note that the statistics for the North East Atlantic are limited to a small number of available observations (18, see Table 1).

3.3. Temperature dependence of P_m^B

Temperature dependence of the photosynthetic parameters has been assessed in several studies. In particular, Eppley (1972), Behrenfeld and Falkowski (1997), Finenko et al. (2002) and Bouman et al. (2005) all report an exponential increase of the assimilation number with temperature, at least up to 20 °C. The dataset used by Bouman et al. (2005) (which is a subset of the one used in our study) displays a decrease after 20 °C corresponding to measurements taken mainly in the Arabian Sea. Exponential, monotonically-increasing models such as that of Eppley (1972) fail to reproduce the observed trend at high temperature.

Fig. 6 illustrates the behaviour of the two models according to temperature. Up to 9 °C the assimilation number lies between 0 and 5 mg C (mg Chl)$^{-1}$ h^{-1}. Both models perform well in this temperature range except for a few measured assimilation number that are very low (smaller than 0.5 mg C (mg Chl)$^{-1}$ h^{-1}). For temperatures in the range 9 to 20 °C both models underestimate the measurements. Despite their ability to reproduce the almost linear increase observed in the in situ data, the models exhibit a strong bias (smaller for the LTB model). Again, a small number of in situ measurements (P_m^B < 3 mg C(mg Chl)$^{-1}$ h^{-1} and 14 < temperature < 20 °C) behave very differently from the rest. It is interesting to note that these were sampled in the North East Atlantic in October whereas the great majority of the other measurements in the same temperature range were taken in the North West Atlantic between October and November.

For temperatures above 20 °C, measurements were taken mostly from the Arabian Sea. One can observe a large variability that is independent of temperature. Bouman et al. (2005) attribute this variability to the taxonomic composition observed in the Arabian Sea. Both models fall within the observed range of assimilation numbers. However the LTB model manages to reproduce a broader range of the variability than the LTN model.

4. Application to remote-sensing data

The two models presented in Sections 2.1.1 and 2.1.2 have shown some promising results when compared point-to-point against in situ data collected during a large number of cruises. This section presents the results of the two models when applied to climatological remote-

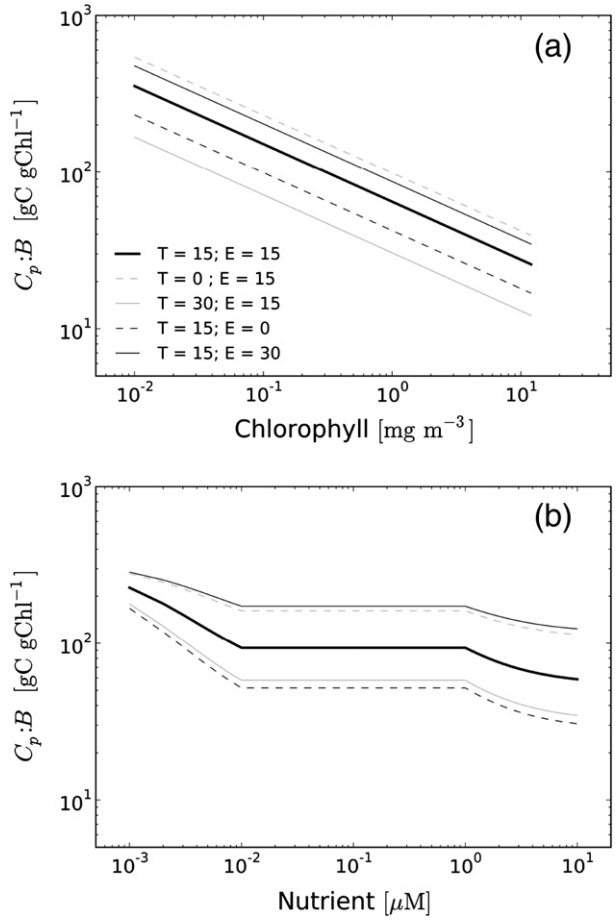

Fig. 3. Carbon-to-chlorophyll ratio as defined in the LTB model (a), plotted as a function of chlorophyll; as defined in the LTN model (b), plotted as a function of nutrient concentration. Units are as follow: T in °C; E in mol quanta m^{-2} d^{-1}.

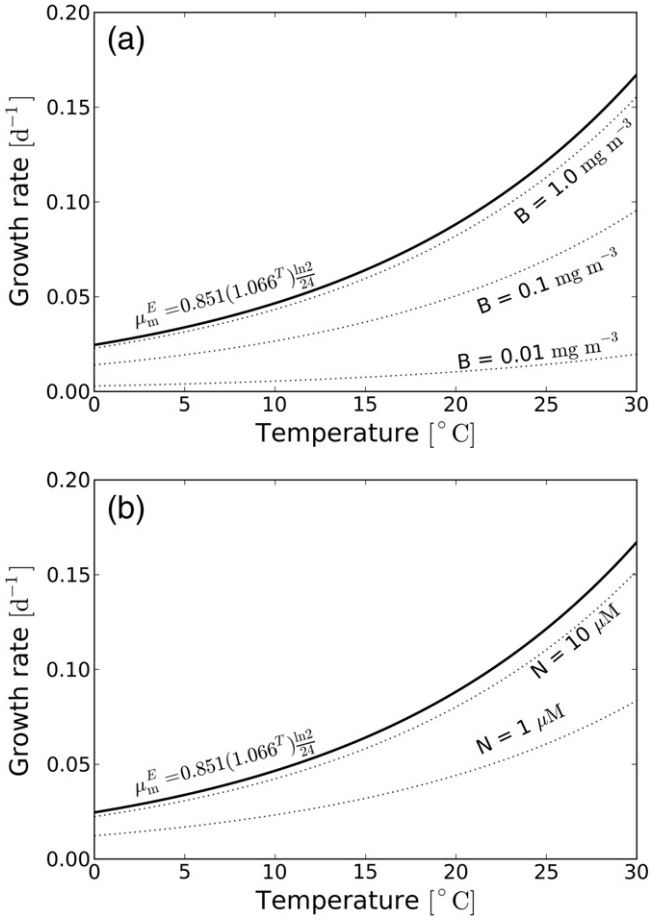

Fig. 4. Maximum realised growth rate, defined in the LTB model (a), and LTN model (b), for varying concentration of biomass. μ_m^E represents the maximum growth rate defined in Eppley (1972).

sensing data. The first step was to apply the models on two regions to compare the results qualitatively with the in situ data. The second step was to apply the models at the global scale.

4.1. Application to the North West Atlantic and the Arabian Sea

Because of the mismatch in time between the satellite data and the in situ data (most of the in situ data were collected prior to 1997, when SeaWiFS was launched), we are not in a position to validate the satellite estimates of P_m^B directly. Instead, we examine whether the values obtained regionally using climatologies of satellite data are qualitatively similar to the in situ P_m^B values for a given region and a given month. We have chosen the regions and the months to correspond to areas and periods for which most in situ data are available. Note that Bouman et al. (2005) showed that a temperature-based model for predicting P_m^B worked well for the North West Atlantic, but not for the Arabian Sea. Hence the choice of these two regions for the comparison is also designed to examine whether the inclusion of additional environmental variables in the model has helped improve the predictions in the Arabian Sea.

As in Section 2.3, the de Boyer Montégut et al. (2004) climatology of mixed-layer depth and the Garcia et al. (2006) climatology of surface nitrate were used. The rest of the input data were provided by various climatologies of remotely-sensed data:

- SeaWiFS monthly climatology of photosynthetically-active radiation
- SeaWiFS monthly climatology of surface chlorophyll concentration
- MODIS monthly climatology of sea-surface temperature

All the above data are available at http://oceancolor.gsfc.nasa.gov/. They are provided at 9 km resolution and down-scaled to 90 km, to save computational time.

Two regions are then extracted: the North West Atlantic (between 40 and 60°N and 45 and 70°W) and the Arabian Sea (between 5 and 30°N and 50 and 70°E). These two regions were chosen because they cover most of the in situ data available (see Fig. 1).

Results of the two models are analysed as a function of temperature (as in Bouman et al., 2005) to highlight the variability associated with temperature, but also the variability that is not associated with temperature, in the Arabian Sea in particular. The result for each month is plotted separately and the in situ measurements for the corresponding month and region are overlaid. Fig. 7 shows the results for four months. These four months have been selected because they yield most of the in situ data for comparison.

As previously noted, the general trend of the assimilation number plotted as a function of temperature is quasi-linear for temperatures below 20 °C. However, there is a marked difference between the two models: The LTN model generally gives lower values than the LTB model in both regions and as the temperature increases, the difference between the two models increases slightly. In the North West Atlantic, both models are within the range of variation of the in situ measurements. In the Arabian Sea, the LTB model gives more realistic values (in particular in November when the LTN model underestimates the observations).

When applied to remote-sensing climatologies, the two models show some differences and some similarities. One possible explanation is that the differences arise from the nutrient fields, which are used as input to the LTN model but not to the LTB model. According to Fig. 2,

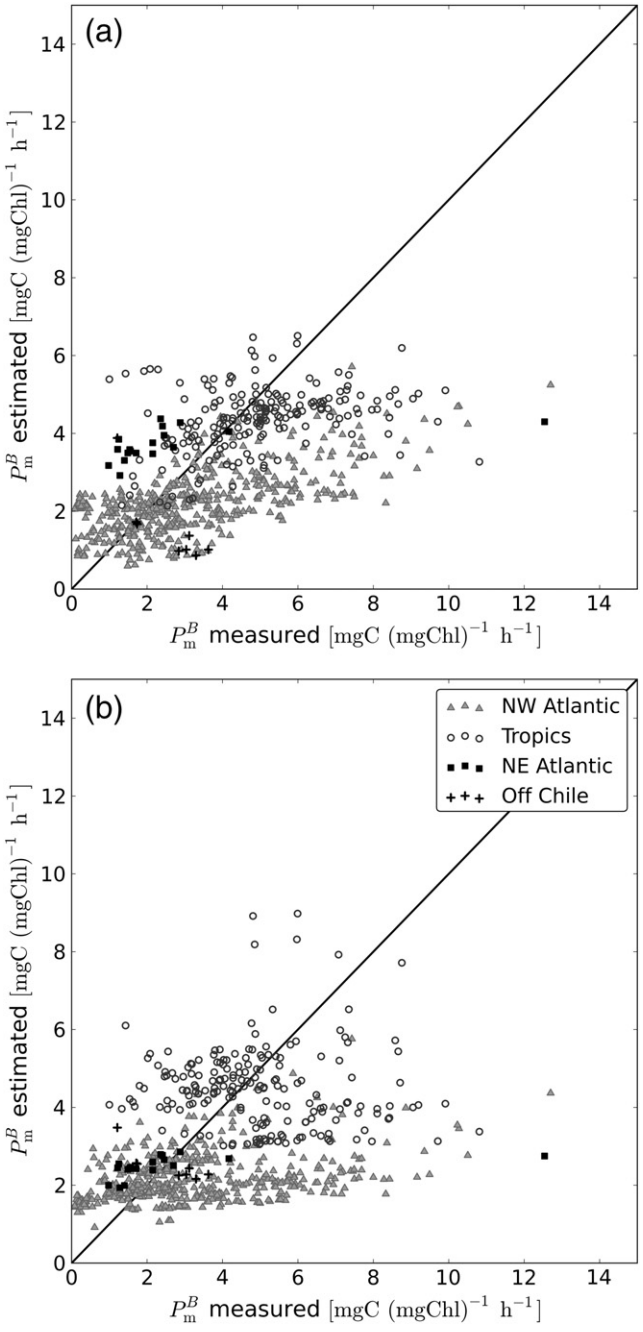

Fig. 5. Comparison between in situ and modelled P^B_m (a: LTB model, b: LTN model).

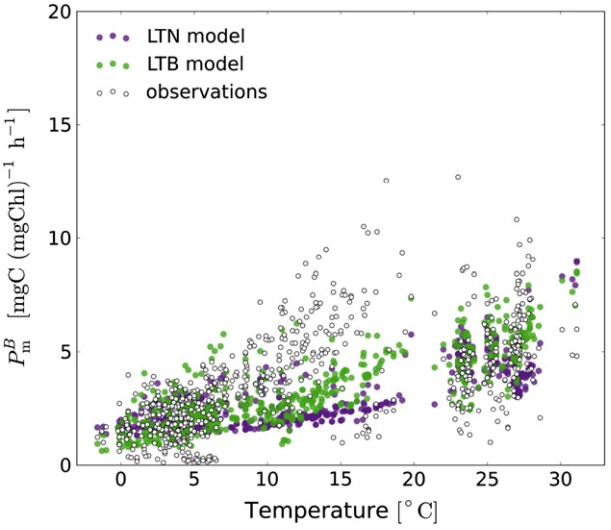

Fig. 6. Temperature dependency of P^B_m.

Table 3
Bias, root mean square error (RMSE) and Spearman correlation coefficient (r) of the comparisons between in situ and modelled assimilation number for both LTN and LTB models.

Area	Model	Bias	RMSE	r	p-Value
North West Atlantic	LTN	−1.105	2.281	0.34	0.11
	LTB	−0.765	1.866	0.58	$<10^{-3}$
North East Atlantic	LTN	−0.089	2.435	0.73	$<10^{-3}$
	LTB	1.60	2.800	0.72	$<10^{-3}$
Tropics	LTN	−0.481	2.244	−0.18	0.28
	LTB	0.196	1.865	0.35	0.15
All	LTN	−0.889	2.265	0.37	0.06
	LTB	−0.43	1.898	0.45	0.05

the sensitivity of the LTN model to light changes with the nutrient concentration, becoming more important at high nutrient concentrations. In the North West Atlantic box (see Fig. 1), the mean nutrient concentrations during May and November are similar and rather high (3.01 and 2.6 μM respectively) according to the World Ocean Atlas climatology used here. This makes the LTN model very sensitive to the light level. In May and November the average light level in the mixed layer are quite different (2.6 and 12.0 mol quanta m^{-2} d^{-1} respectively), leading to the large differences in the LTN model outputs in May and November. The LTB model uses instead the chlorophyll fields, with mean values of 1.1 and 0.70 mg m^{-3} for May and November respectively. At these concentrations, the sensitivity of the LTB model to light is relatively low.

4.2. Global distribution

Measurements of the assimilation number are not available for most of the global ocean for comparison, but nevertheless it is interesting to look at the results of the two models at large scales. Here we offer a visual comparison of the two models at the global scale (see Fig. 8). The same climatological dataset as in Section 4.1 has been used and two contrasting months are shown (May and December).

Throughout the year, the highest values are generally observed in the tropics. In May we observe higher values in the northern hemisphere, whereas in December, the highest values are observed in the southern hemisphere. Despite the marked differences between the two models in absolute values, we note some similarities in the patterns.

The sensitivity plot in Fig. 2 shows that very low nutrient concentrations together with high temperatures lead to high assimilation numbers for the LTN model (irrespective of the light level). All these conditions are met in the northern hemisphere in May and in the southern gyres in December, so it is not surprising to find the highest values in these regions. The LTN model also exhibits very low values in high latitudes, which is related to high nutrient concentrations producing low carbon-to-chlorophyll ratio (see Fig. 3b). High P^B_m observed in the Gulf of Mexico and in the Arabian Sea in May, for example, are due to elevated temperatures inducing high values of maximum growth rate in combination with high light level producing high carbon-to-chlorophyll ratio.

On the other hand, the range of variation of the LTB model is much smaller, with values between 3 and 12 mg C (mg Chl)$^{-1}$ h^{-1} which is more conservative. One can note a relatively good agreement between models in large-scale patterns. However, some marked differences are observed. For instance, in the southern hemisphere gyres (particularly in the Pacific Ocean in December), the LTB model produces

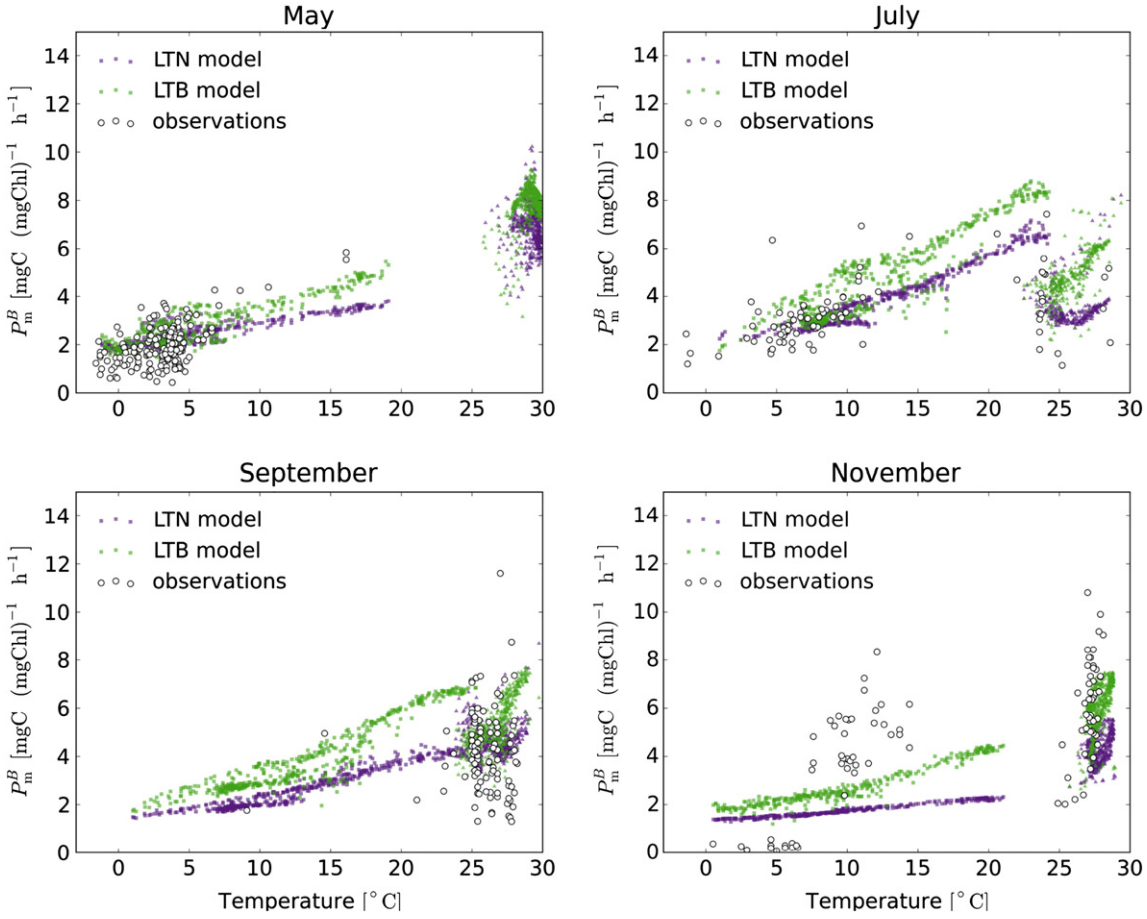

Fig. 7. Climatological satellite estimate of P_m^B as a function of temperature in the North West Atlantic (squares) and in the Arabian Sea (triangles).

a patch of lower P_m^B which is the result of the nutrient limitation term μ' (see Fig. 4). This may appear counter-intuitive because one would expect small phytoplankton cells in these very oligotrophic waters, and therefore high P_m^B. One should note that no measurements were available in very oligotrophic waters, and therefore the LTB model may not be accurate in those conditions.

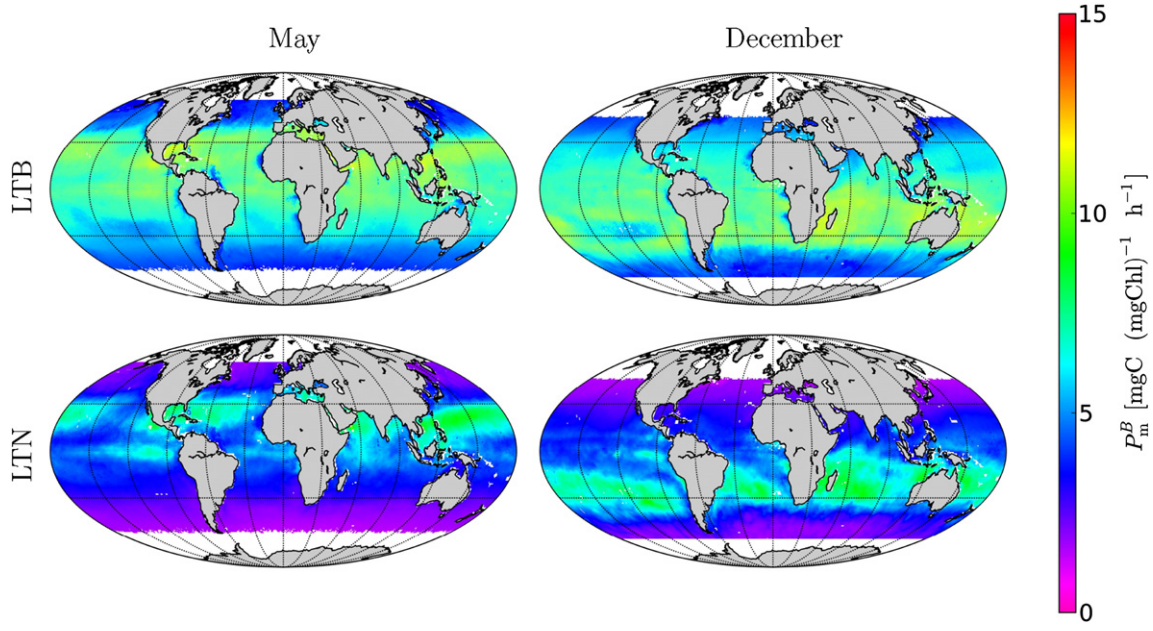

Fig. 8. Global estimates of P_m^B from satellite climatologies from the LTB (top) and LTN (bottom) model for the months of May (left) and December (right).

5. Discussion

Estimation of primary production at large spatial scales has often relied on large databases of the photosynthesis-light parameters. Longhurst et al. (1995) divided the ocean into four biogeochemical domains and prescribed the photosynthesis-light parameters by selecting characteristic values for each domain by season. Platt et al. (2008) designed the nearest-neighbour methodology, which is a data-intensive method that requires a large database of parameters for its regional implementation. The main advantage of the two models considered here is that they estimate assimilation number based on easily-measured environmental variables, with the potential to be applied globally, as demonstrated here.

The LTN model implemented here is a direct application at global scale of the model of Cloern et al. (1995). Despite the fact that this model is not tuned to the in situ data on P^B_m used here, it gives good results (Table 3) in some areas of the world (for example in the North West Atlantic) when compared with the in situ data. The higher RMSEs in some other regions (e.g. the tropics) may be a consequence of having had to use climatological values for surface irradiance, in combination with the high sensitivity of the model to light at high nutrient levels. When implemented globally, some unrealistically low values were obtained at high latitudes, resulting from a combination of relatively lower light level and higher nutrient availability. Implementing the LTN model by remote sensing would require that we find a remote sensing proxy for nutrients, if the climatological nutrient fields were considered not to be acceptable. In fact, algorithms have been developed for some regions (for example in the North Pacific and North West Atlantic Oceans) where surface nitrate concentrations are derived from surface temperatures and chlorophyll concentrations (Goes, Gomes, Saino, Wong, & Mordy, 2004; Goes et al., 2000; Sathyendranath et al., 1991). One could also rely on biogeochemical models for the nutrient fields, provided the models were suitably validated for the application.

The LTB model, on the other hand, provides better estimates of P^B_m when compared with in situ data. This is confirmed when we apply the model to satellite climatologies (see Section 4). This may be explained by the availability of all required input data for this model directly from remote sensing. The LTB model should, however, be applied with caution: most of the data used in the optimisation/validation have been collected in two regions of the world: the North West Atlantic and the Arabian Sea. It would therefore need to be further validated for other regions, particularly in very oligotrophic regions.

A critical variable, used by both models, is the mixed-layer depth (for computation of average light in the layer), which cannot be estimated on a global scale in an operational mode from remote-sensing data. For this quantity we rely on climatologies or hydrodynamic models.

Both models use the daily average light in the mixed layer of which the computation relies on an underwater light-transmission model to estimate the diffuse attenuation coefficient (K_d) for photosynthetically-active radiation. In this study we used the model of Sathyendranath and Platt (1988) which was designed for case 1 waters. Application to case 2 waters requires that the model be adapted to include contributions to K_d from in-water constituents that vary independently of phytoplankton such as sediment and yellow substances. Other methods to estimate the diffuse attenuation coefficient for photosynthetically-active radiation from remote sensing also exist (e.g., Lee et al., 2005, for application to coastal waters and the open ocean) and may be used in this context.

6. Conclusion

In this paper, we have presented two models to estimate the assimilation number of marine phytoplankton at the global scales: one parameterised using culture data, and the other, similar in concept, parameterised using in situ data from photosynthesis–irradiance experiments. The model of Cloern et al. (1995) performs remarkably well, considering that it is based on laboratory measurements. The alternative model presented here is parameterised using in situ data, and uses chlorophyll rather than nutrients as an input variable, to facilitate implementation with remotely-sensed data. It performs better than the model of Cloern et al. (1995) when compared with observations, but this will need to be confirmed with independent data from regions not represented in the in situ database.

Potential applications of these models include estimation of primary production at large spatial scales using remotely-sensed data. For this purpose, the initial slope of the photosynthesis–irradiance curve (generally referred to as α^B) will also need to be estimated at the same temporal and spatial resolution. The simplest approach is to relate the initial slope to the assimilation number (Rey, 1991). Another approach was suggested by Kasai, Hiroaki, and Atsushi (1998) who related α^B to the assimilation number and the surface irradiance history.

Global estimates of assimilation number are of potential interest also to the marine ecosystem modelling community: in many ecosystem models, photosynthetic parameters are fixed and could be improved using simple models such as the ones presented in this paper.

Acknowledgements

The authors thank the two anonymous reviewers for their constructive comments and James Cloern for his support. The authors also thank the UK NERC Earth Observation Data Acquisition and Analysis Service (NEODAAS) for providing computing facilities and data storage. This study is a contribution to the ESA CoastColour Project and the Ocean-Colour Climate Change Initiative of ESA, to the Indo-MARECLIM Project (EU Project No. 295092) and to the UK NERC National Centre for Earth Observation (NCEO).

References

Antoine, D., André, J. M., & Morel, A. (1996). Oceanic primary production: II. Estimation at global scale from satellite (coastal zone color scanner) chlorophyll. *Global Biogeochemical Cycles*, *10*, 57–69.

Antoine, D., & Morel, A. (1996). Oceanic primary production: I. Adaptation of a spectral light-photosynthesis model in view of application to satellite chlorophyll observations. *Global Biogeochemical Cycles*, *10*, 43–45.

Behrenfeld, M., Boss, E., Siegel, D. A., & Shea, D.M. (2005). Carbon-based ocean productivity and phytoplankton physiology from space. *Global Biogeochemical Cycles*, *19* (14 pp.).

Behrenfeld, M. J., & Falkowski, P. G. (1997). Photosynthetic rates derived from satellite-based chlorophyll concentration. *Limnology and Oceanography*, *42*, 1–20.

Bouman, H. A., Platt, T., Sathyendranath, S., & Stuart, V. (2005). Dependence of light-saturated photosynthesis on temperature and community structure. *Deep-Sea Research Part I*, *52*, 1284–1299.

Brewin, R. J. W., Sathyendranath, S., Hirata, T., Lavender, S. J., Barciela, R. M., & Hardman-Mountford, N. J. (2010). A three-component model of phytoplankton size class for the Atlantic Ocean. *Ecological Modelling*, *221*, 1472–1483.

Chavez, F. P., Messié, M., & Pennington, J. T. (2011). Marine primary production in relation to climate variability and change. *The Annual Review of Marine Science*, *3*, 227–260.

Cloern, J. E., Grenz, C., & Vidergar-Lucas, L. (1995). An empirical model of the phytoplankton chlorophyll: Carbon ratio—The conversion factor between productivity and growth rate. *Limnology and Oceanography*, *40*, 1313–1321.

de Boyer Montégut, C., Madec, G., Fisher, A. S., Lazar, A., & Iudicone, D. (2004). Mixed layer depth over the global ocean: An examination of profile data and profile-based climatology. *Journal of Geophysical Research*, *109*, C12003.

Eppley, R. W. (1972). Temperature and phytoplankton growth in the sea. *Fishery Bulletin*, *70*.

Finenko, Z. Z., Churilova, T. Y., Sosik, H. M., & Basturk, O. (2002). Variability of photosynthetic parameters of the surface phytoplankton in the Black Sea. *Oceanology*, *42*, 53–67.

Friedrichs, M.A., Carr, M. -E., Barber, R. T., Scardi, M., Antoine, D., Armstrong, R. A., et al. (2009). Assessing the uncertainties of model estimates of primary productivity in the tropical Pacific Ocean. *Journal of Marine Systems*, *76*, 113–133.

Garcia, H. E., Locarnini, R. A., Boyer, T. P., & Antonov, J. I. (2006). Nutrients (phosphate, nitrate, silicate). In S. Levitus (Ed.), *World Ocean Atlas 2005*, *Vol. 4*, Washington, D.C.: NOAA Atlas NESDIS 64, U.S. Government Printing Office.

Geider, R. J. (1987). Light and temperature dependence of the carbon to chlorophyll a ratio in microalgae and cyanobacteria: Implications for physiology and growth of phytoplankton. *New Phytologist*, *106*, 1–34.

Goes, J. I., Gomes, R., do H., R., Saino, T., Wong, C. S., & Mordy, C. W. (2004). Exploiting MODIS data for estimating sea surface nitrate from space. *EOS. Transactions of the American Geophysical Union*, *85*, 449–464.

Goes, J. I., Saino, T., Oaku, H., Ishizaka, J., Wong, C. S., & Nojiri, Y. (2000). Basin scale estimates of sea surface nitrate and new production from remotely sensed sea surface temperature and chlorophyll. *Geophysical Research Letters*, *27*, 1263–1266.

Harrison, W. G., Harris, L. R., & Irwin, B.D. (1996). The kinetics of nitrogen utilization in the oceanic mixed layer: Nitrate and ammonium interactions at nanomolar concentrations. *Limnology and Oceanography*, *41*, 16–32.

Harrison, W. G., & Platt, T. (1980). Variations in assimilation number of coastal marine phytoplankton: Effects of environmental co-variates. *Journal of Plankton Research*, *2*, 249–260.

Hirata, T., Aiken, J., Hardman-Mountford, N., Smyth, T. J., & Barlow, R. G. (2008). An absorption model to determine phytoplankton size classes from satellite ocean colour. *Remote Sensing of Environment*, *112*, 3153–3159.

Huot, Y., Babin, M., & Bruyant, F. (2013). Photosynthetic parameters in the Beaufort Sea in relation to the phytoplankton community structure. *Biogeosciences*, *10*, 3445–3454.

Kasai, H., Hiroaki, S., & Atsushi, T. (1998). Estimation of standing stock of chlorophyll a and primary production from remote-sensed ocean color in the Oyashio region, the Western subarctic Pacific, during the spring bloom in 1997. *Journal of Oceanography*, *54*, 527–537.

Lee, Z. -P., Darecki, M., Carder, K. L., Davis, C. O., Stramski, D., & Rhea, W. J. (2005). Diffuse attenuation coefficient of downwelling irradiance: An evaluation of remote sensing methods. *Journal of Geophysical Research*, *110*, 1–9.

Longhurst, A., Sathyendranath, S., Platt, T., & Caverhill, C. (1995). An estimate of global primary production in the ocean from satellite radiometer data. *Journal of Plankton Research*, *17*, 1245–1271.

Marañón, E., & Holligan, P.M. (1999). Photosynthetic parameters of phytoplankton from 50°N to 50°S in the Atlantic Ocean. *Marine Ecology Progress Series*, *176*, 191–203.

Platt, T., & Sathyendranath, S. (1999). Spatial structure of pelagic ecosystem processes in the global ocean. *Ecosystems*, *2*, 384–394.

Platt, T., Sathyendranath, S., Forget, M. -H., White, G. N., III, Caverhill, C., Bouman, H., et al. (2008). Operational estimation of primary production at large geographical scales. *Remote Sensing of Environment*, *112*, 3437–3448.

Rey, F. (1991). Photosynthesis–irradiance relationships in natural phytoplankton populations of the Barents Sea. In E. Sakshaug, C. C. Hopkins, & N. A. Øritsland (Eds.), *Proceedings of the Pro Mare Symposium on Polar Marine Ecology, Trondheim, 12–16 May, 1990. Polar research, Vol. 10*. (pp. 105–116).

Sathyendranath, S., & Platt, T. (1988). The spectral irradiance field at the surface and in the interior of the ocean: A model for applications in oceanography and remote sensing. *Journal of Geophysical Research*, *93*, 9270–9280.

Sathyendranath, S., Platt, T., Horne, E. P. W., Harrison, W. G., Ulloa, O., Outerbridge, R., et al. (1991). Estimation of the new production in the ocean by compound remote sensing. *Nature*, *253*, 129.

Sathyendranath, S., Stuart, V., Nair, A., Oka, K., Nakane, T., Bouman, H., et al. (2009). Carbon-to-chlorophyll ratio and growth rate of phytoplankton in the sea. *Marine Ecology Progress Series*, *383*, 73–84.

Sheskin, D. J. (2007). *Handbook of parametric and nonparametric statistical procedure* chapter. The Mann–Whitney U test (4th ed.). : Chapman & Hall/CRC, Taylor and Francis Group, 532–539.